



|                  |  |
|------------------|--|
| Title            | A rigorous definition of nonlinear parameter $\gamma$ and effective area $A_{\text{eff}}$ for photonic crystal optical waveguides  |
| Author(s)        | Sato, Takanori; Makino, Shuntaro; Ishizaka, Yuhei; Fujisawa, Takeshi; Saitoh, Kunimasa   |
| Citation         | Journal of the Optical Society of America B, 32(6), 1245-1251<br><a href="https://doi.org/10.1364/JOSAB.32.001245">https://doi.org/10.1364/JOSAB.32.001245</a>   |
| Issue Date       | 2015-06-01   |
| Doc URL          | <a href="http://hdl.handle.net/2115/67118">http://hdl.handle.net/2115/67118</a>  |
| Rights           | © 2015 Optical Society of America. One print or electronic copy may be made for personal use only. Systematic reproduction and distribution, duplication of any material in this paper for a fee or for commercial purposes, or modifications of the content of this paper are prohibited. |
| Type             | article (author version)   |
| File Information | 235776.pdf   |



[Instructions for use](#)

# A rigorous definition of nonlinear parameter $\gamma$ and effective area $A_{\text{eff}}$ for photonic crystal optical waveguides

TAKANORI SATO,\* SHUNTARO MAKINO, YUHEI ISHIZAKA, TAKESHI FUJISAWA, KUNIMASA SAITOH

Graduate School of Information Science and Technology, Hokkaido University North 14, West 9, Kita-ku, Sapporo 060-0814, Japan  
\*Corresponding author: tsato@icp.ist.hokudai.ac.jp

Received XX Month XXXX; revised XX Month, XXXX; accepted XX Month XXXX; posted XX Month XXXX (Doc. ID XXXXX); published XX Month XXXX

**A rigorous definition of nonlinear parameter  $\gamma$  for high-index-contrast (HIC) periodic optical waveguides, such as photonic crystal (PC) optical waveguides, is proposed. The definition is fully vectorial, and approximations assumed in previous works are unnecessary. The  $\gamma$  values calculated by the proposed definition are compared with those obtained by previous definitions, the rigorous nonlinear mode solver, and measured values for weakly guiding optical fibers, HIC Si-nanowire waveguides, and PC waveguides. It is demonstrated that the  $\gamma$  values calculated by proposed definition agree well with those of the rigorous nonlinear mode solver and experiments for all three waveguides, showing the validity of the definition. © 2015 Optical Society of America**

**OCIS codes:** (190.0190) Nonlinear optics; (190.3270) Kerr effect; (130.5296) Photonic crystal waveguides.

<http://dx.doi.org/10.1364/AO.99.099999>

## 1. INTRODUCTION

Nonlinear optical effects, including second-order and third-order nonlinearities, are promising optical effects for the high-speed and low-energy operation of optical communication devices. Second-order nonlinearities, such as second-harmonic generation (SHG) [1,2] and Pockels effect [3,4] in the photonic crystal (PC) structure have been reported. Third-order nonlinearities, such as self-phase modulation (SPM) [5–14], cross-phase modulation (XPM) [8,9,12–14], two-photon absorption (TPA) [8–10,12–14], three-photon absorption (ThPA) [8,12,14], and four-wave mixing (FWM) [8–10,13–15] have received attention as being key for all-optical signal processing. For the evaluation of third-order nonlinear characteristics in optical waveguides, a nonlinear parameter  $\gamma$ , which is defined in the nonlinear Schrödinger equation (NLSE), has been widely used [8,14,16].  $\gamma$  is mainly related to SPM, whereas some of the third-order nonlinear phenomena, including XPM, ThPA and FWM, can also be evaluated by  $\gamma$  [12,14,16,17]. There are two ways to evaluate  $\gamma$  theoretically: (i) calculate the nonlinear phase shift by directly solving the nonlinear Maxwell's equation self-consistently using the nonlinear mode solver [18,19] and (ii) calculate the effective area,  $A_{\text{eff}}$  of the “linear” optical waveguide and use the definition  $\gamma = k_0 n_2 / A_{\text{eff}}$  [14], where  $k_0$  is the free-space wavenumber and  $n_2$  is the nonlinear refractive index. The method (i) seems to be physically more

rigorous than method (ii) and has been used to evaluate the nonlinear phase shift of uniform and periodic optical waveguides. However, iteration is necessary to obtain converged solutions, resulting in huge computational cost. Therefore, method (ii) has been widely used to evaluate  $\gamma$  because only linear guided mode analysis is necessary. This method has been used for uniform structures, such as optical fibers and Si-nanowire waveguides, and has also been adapted to non-uniform structures, such as photonic crystal waveguides. In PC waveguides, because the waveguide structure varies along the propagation direction in one period of the waveguide,  $A_{\text{eff}}$  is also varied along the propagation direction. To evaluate  $\gamma$  of PC waveguides, variations of  $A_{\text{eff}}$  along the propagation direction have to be carefully treated. Many definitions of  $\gamma$  for PC waveguides have been reported, as shown in Table 1 (Methods B, C, and D). The methods are different each other in terms of the definition of  $A_{\text{eff}}$  and the use of slowdown factor  $S$  [20]. In [12], the weakly guiding approximation was used for  $A_{\text{eff}}$  (Method B). In [15],  $A_{\text{eff}}$  is calculated by the modal volume [21,22],  $V_{\text{eff}}$ , which was originally defined for the resonator analysis and has no direct relation to NLSE (Method C). In [23] (Method D-1) and [24] (Method D-2), so-called slowdown factor  $S$  is multiplied to  $\gamma$  obtained by Methods B and C. Because the  $\gamma$  values calculated by these methods are different, it is not certain whether these assumptions are appropriate for HIC periodic waveguides. Hence, a rigorous formalism is required to accurately evaluate  $\gamma$ , especially for PC waveguides.

**Table 1. List of definitions of  $\gamma$ ,  $\gamma_{\text{eff}}$  and  $A_{\text{eff}}$  for uniform and PC waveguides.**

| Calculation Method       | Description   | Used Equations | References |
|--------------------------|---|----------------|------------|
| (For uniform waveguides) |   |                |            |
|                          | Derived from vectorial-based NLSE.  | (5), (6)       | [16]       |
| (For PC waveguides)      |   |                |            |
| Method A (proposed)      | Derived from vectorial-based NLSE.  | (10), (11)     | This work  |
| Method B                 | Weakly guiding approximation is adapted to Method A.                      | (14), (15)     | [12]       |
| Method C                 | Calculated value that is estimated by the modal volume $V_{\text{eff}}$ . | (16), (17)     | [15]       |
| Method D-1               | Estimated by Method B and the slowdown factor $S$ .                       | (15), (18)     | [23]       |
| Method D-2               | Estimated by Method C and the slowdown factor $S$ .                       | (17), (19)     | [24]       |
| Method E                 | Calculated by nonlinear modal analysis.                                   | (20), (21)     | [19]       |
| Method F                 | Measured value obtained by SPM-induced spectral broadening analysis.      | (22)           | [5,14]     |

In this paper, we propose a new definition of  $\gamma$  based on the vectorial formulation for HIC periodic waveguides. We first describe the proposed and previous definitions of  $\gamma$  briefly in Section 2. Next, we compare the values of  $\gamma$  obtained by the proposed definition and conventional definitions for an optical fiber, a Si-nanowire waveguide, and dispersion engineered PC waveguides using the three-dimensional (3D) finite element method (FEM) [19]. From the numerical results presented in Section 3, it is demonstrated that  $\gamma$  values calculated by the proposed definition agree well with those obtained by the nonlinear mode solver and the experiment for all three waveguide structures (weakly guiding, strongly guiding, and strongly guiding periodic waveguides), showing the validity of the definition.

## 2. THEORY AND EVALUATION FORMULA

Here, we review the derivation of  $\gamma$  from NLSE in full-vectorial form [16] and apply equations of [16] to the case of periodic optical waveguides. Additionally, conventionally used  $\gamma$  definitions for periodic optical waveguides are briefly summarized.

### A. Definition of $\gamma$ by Vectorial-Based NLSE.

In this paper, the situation of a monochromatic wave propagating in single-mode waveguides is assumed for the derivation of NLSE to explicitly demonstrate the validity of our proposed definition; therefore, the relevant nonlinear effect is SPM only. A slowly varying envelope approximation is assumed, and the electric field vector  $\mathbf{E}(\mathbf{r}, t)$  and the magnetic field vector  $\mathbf{H}(\mathbf{r}, t)$  propagating along the  $z$ -direction are expressed as:

$$\mathbf{E}(\mathbf{r}, t) = \frac{1}{2} \left[ A(z, t) \mathbf{e}(x, y, \omega) \exp\{j(\omega t - \beta z)\} + \text{c.c.} \right], \quad (1)$$

$$\mathbf{H}(\mathbf{r}, t) = \frac{1}{2} \left[ A(z, t) \mathbf{h}(x, y, \omega) \exp\{j(\omega t - \beta z)\} + \text{c.c.} \right], \quad (2)$$

where  $A(z, t)$  is the electromagnetic field envelope,  $\mathbf{e}(x, y, \omega)$  and  $\mathbf{h}(x, y, \omega)$  are the normalized transverse-electric and transverse-

magnetic field distributions, and  $\beta$  is the propagation constant of the mode at frequency  $\omega$ . The abbreviation ‘‘c.c.’’ stands for complex conjugate. Setting  $A(z, t) = P^{1/2}$  (const.) results in the continuous wave (CW) case where  $P$  is the optical power. Without scalar approximation, vectorial NLSE is derived as [16]

$$\frac{\partial A}{\partial z} + \beta_1 \frac{\partial A}{\partial t} - j \frac{1}{2} \beta_2 \frac{\partial^2 A}{\partial t^2} = -j\gamma |A|^2 A, \quad (3)$$

where  $\beta_n$  ( $n = 1, 2$ ) is the  $n$ -th order differential value of  $\beta$ . The nonlinear parameter  $\gamma$  is defined as

$$\gamma = k_0 \frac{\epsilon_0}{\mu_0} \frac{\int_{-\infty}^{\infty} \int_{-\infty}^{\infty} n_0^2 n_2 |\mathbf{e}|^4 dx dy}{\left| \int_{-\infty}^{\infty} \int_{-\infty}^{\infty} \text{Re}[\mathbf{e} \times \mathbf{h}^*] \cdot \mathbf{i}_z dx dy \right|^2}, \quad (4)$$

where  $\epsilon_0$  and  $\mu_0$  are the permittivity and permeability in vacuum,  $n_0$  is the refractive index,  $*$  denotes the complex conjugate, and  $\mathbf{i}_z$  is the unit vector directed along the  $z$ -direction.  $\text{Re}[\ ]$  stands for the real part. As seen in Eq. (3),  $\gamma$  indicates the amount of nonlinear phase shift per propagation length and per propagation power. If a waveguide contains only one nonlinear material that has a large nonlinear refractive index  $n_2$ , Eq. (4) can be rewritten with the effective area  $A_{\text{eff}}$  as

$$\gamma = \frac{k_0 n_2}{A_{\text{eff}}}, \quad (5)$$

$$A_{\text{eff}} = \frac{\mu_0}{\epsilon_0} \frac{\left| \int_{-\infty}^{\infty} \int_{-\infty}^{\infty} \text{Re}[\mathbf{e} \times \mathbf{h}^*] \cdot \mathbf{i}_z dx dy \right|^2}{\iint_{\text{NL}} n_0^2 |\mathbf{e}|^4 dx dy}, \quad (6)$$

where the description ‘‘NL’’ denotes the area of the nonlinear material.

We now consider non-uniform periodic waveguides, including PC waveguides, which have variations of the transverse field distributions  $\mathbf{e}$  and  $\mathbf{h}$  along the  $z$ -direction. Therefore, the nonlinear parameter  $\gamma$  should be expressed as a function of  $z$ . Figures 1 (a) and (b) show the schematics of a line-defect PC waveguide and the electric field distribution  $|\mathbf{e}|$  in the  $xz$ -plane and  $xy$ -plane, respectively. As seen in Figs. 1 (a) and (b),  $|\mathbf{e}|$  distributions at  $z = 0$  and  $z = a/2$  are remarkably different, where  $a$  is one period length of the PC waveguides. Figures 1 (c) and (d) show the  $A_{\text{eff}}$  and  $\gamma$  of the PC waveguides shown in Fig. 1(a) calculated by (6) and (5) as a function of  $z$ , respectively. The  $z$ -dependence of  $A_{\text{eff}}$  and  $\gamma$  is clearly seen, and careful treatment of the nonlinear phase shift variations is required. In the PC waveguides, we can consider that the nonlinear phase shift is periodically modulated along the  $z$ -direction. From the physical meaning of  $\gamma$ , the total amount of the nonlinear phase shift in one period of PC waveguides can be expressed as

$$\Delta\phi = P \int_z^{z+a} \gamma(z) dz = Pa\gamma^{\text{PC}}, \quad (7)$$

where  $\gamma^{\text{PC}}$  is equivalent to the mean value of  $\gamma(z)$  [25]. Using Eq. (4) as  $\gamma(z)$ , we find the new definition of the nonlinear parameter for HIC periodic optical waveguides as

$$\begin{aligned} \gamma^{\text{PC}} &= \frac{1}{a} \int_z^{z+a} k_0 \frac{\epsilon_0}{\mu_0} \frac{\int_{-\infty}^{\infty} \int_{-\infty}^{\infty} n_0^2 n_2 |\mathbf{e}|^4 dx dy}{\left| \int_{-\infty}^{\infty} \int_{-\infty}^{\infty} \text{Re}[\mathbf{e} \times \mathbf{h}^*] \cdot \mathbf{i}_z dx dy \right|^2} dz \\ &= \frac{a}{\left| \int_z^{z+a} dz \right|^2} k_0 \frac{\epsilon_0}{\mu_0} \frac{\int_z^{z+a} \left[ \int_{-\infty}^{\infty} \int_{-\infty}^{\infty} n_0^2 n_2 |\mathbf{e}|^4 dx dy \right] dz}{\left| \int_{-\infty}^{\infty} \int_{-\infty}^{\infty} \text{Re}[\mathbf{e} \times \mathbf{h}^*] \cdot \mathbf{i}_z dx dy \right|^2} \end{aligned}$$

$$= k_0 a \frac{\epsilon_0}{\mu_0} \frac{\int_z^{z+a} \int_{-\infty}^{\infty} \int_{-\infty}^{\infty} n_0^2 n_2 |\mathbf{e}|^4 dx dy dz}{\left| \int_z^{z+a} \int_{-\infty}^{\infty} \int_{-\infty}^{\infty} \text{Re}[\mathbf{e} \times \mathbf{h}^*] \cdot \mathbf{i}_z dx dy dz \right|^2}, \quad (8)$$

where we use the relationship

$$a = \int_z^{z+a} dz \quad (9)$$

and the optical power is assumed constant. If the waveguide contains only one nonlinear material that has a large nonlinear refractive index  $n_2$ , Eq. (8) can be rewritten as

$$\gamma^{\text{PC}} = \frac{k_0 n_2}{A_{\text{eff}}^{\text{PC}}}, \quad (10)$$

$$A_{\text{eff}}^{\text{PC}} = \frac{1}{a} \frac{\mu_0}{\epsilon_0} \frac{\left| \int_z^{z+a} \int_{-\infty}^{\infty} \int_{-\infty}^{\infty} \text{Re}[\mathbf{e} \times \mathbf{h}^*] \cdot \mathbf{i}_z dx dy dz \right|^2}{\int_z^{z+a} \int_{\text{NL}} n_0^2 |\mathbf{e}|^4 dx dy dz}. \quad (11)$$

For uniform structures, Eqs. (8), (10), and (11) are reduced to Eqs. (4), (5), and (6), respectively. Eq. (8) seems to be the most rigorous evaluation formula for the  $\gamma$  of PC waveguides. If we apply the weakly guiding approximation to Eq. (8), it is reduced to one of the definitions of  $\gamma$  in previous works [12,23], as shown in following Section 2-B.

### B. $\gamma$ Calculated by $A_{\text{eff}}$ with the Weakly Guiding Approximation.

Applying the weakly guiding approximation to Eq. (6), we can obtain the well-known definition of the nonlinear parameter and effective area as [14]

$$\gamma = \frac{k_0 n_2}{A_{\text{eff}}}, \quad (12)$$

$$\tilde{A}_{\text{eff}} = \frac{\left| \int_{-\infty}^{\infty} \int_{-\infty}^{\infty} |\mathbf{e}|^2 dx dy \right|^2}{\int_{-\infty}^{\infty} \int_{-\infty}^{\infty} |\mathbf{e}|^4 dx dy}, \quad (13)$$

where a tilde denotes applying the weakly guiding approximation. We also apply the weakly guiding approximation to Eq. (11) to obtain the previously reported nonlinear parameter and effective area as follows [12,23]:

$$\gamma^{\text{PC}} = \frac{k_0 n_2}{\tilde{A}_{\text{eff}}^{\text{PC}}}, \quad (14)$$

$$\tilde{A}_{\text{eff}}^{\text{PC}} = \frac{1}{a} \frac{\left| \int_z^{z+a} \int_{-\infty}^{\infty} \int_{-\infty}^{\infty} |\mathbf{e}|^2 dx dy dz \right|^2}{\int_z^{z+a} \int_{\text{NL}} |\mathbf{e}|^4 dx dy dz}. \quad (15)$$

For uniform structures, Eqs. (14) and (15) are reduced to Eqs. (12) and (13), respectively.

### C. $\gamma$ Calculated by the Modal Volume.

In some works, the modal volume  $V_{\text{eff}}$  for optical resonators is used to estimate the  $A_{\text{eff}}$  of PC waveguides [15,24]. The nonlinear parameter using  $V_{\text{eff}}$  is given as [15]

$$\gamma^{\text{eff}} = \frac{k_0 n_2}{A_{\text{eff}}^{\text{eff}}}, \quad (16)$$

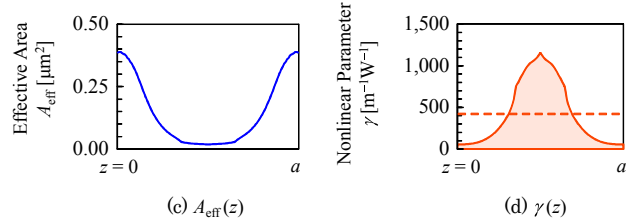
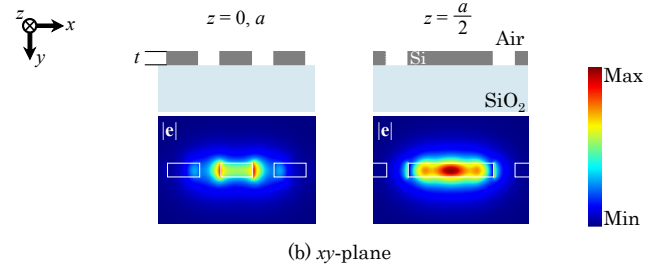
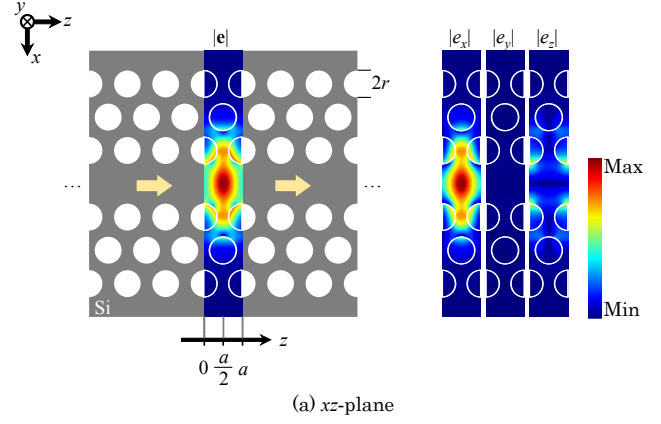


Fig. 1. Schematics of a line-defect PC waveguide and electric field distribution  $|\mathbf{e}|$  in the (a)  $xz$ -plane and (b)  $xy$ -plane, and (c)  $A_{\text{eff}}(z)$  and (d)  $\gamma(z)$ , respectively.  $|e_x|$ ,  $|e_y|$  and  $|e_z|$  denote  $|\mathbf{e} \cdot \mathbf{i}_x|$ ,  $|\mathbf{e} \cdot \mathbf{i}_y|$ , and  $|\mathbf{e} \cdot \mathbf{i}_z|$ . The structural parameters are  $a = 400$  nm,  $r = 0.35a$ ,  $t = 0.45a$ . The linear refractive indices of Si and SiO<sub>2</sub> are 3.48 and 1.45, respectively. The nonlinear refractive index of Si is  $6.0 \times 10^{-18}$  m<sup>2</sup>W<sup>-1</sup>. The number of rows of cladding air holes is 6 for both sides of core.

$$A_{\text{eff}}^{\text{eff}} = \frac{V_{\text{eff}}}{a} \quad \text{with} \quad V_{\text{eff}} = \frac{\iiint n_0^2 |\mathbf{e}|^2 dx dy dz}{n_0^2(\mathbf{r}_{\text{max}}) |\mathbf{e}(\mathbf{r}_{\text{max}})|^2}, \quad (17)$$

where  $\mathbf{r}_{\text{max}}$  denotes the position where  $|\mathbf{e}|$  is at the maximum. We note that the modal volume is not associated with NLSE, and hence,  $\gamma$ , although  $V_{\text{eff}}$  indicates the capability of energy confinement.

### D. Effective Nonlinear Parameter $\gamma_{\text{eff}}$ with Slowdown Factor.

In addition to the above expressions for the nonlinear parameter, other works mention that the slowdown factor  $S$  [20], defined as the ratio of the phase velocity over the group velocity, which is calculated as  $n_g/n_0$ , where  $n_g$  is group index, is required to estimate  $\gamma$  of PC waveguides [11,23,24,26]. In [20], it was pointed out that the value of  $\gamma$  increased with  $n_g$ , and  $S^\xi$  ( $1 < \xi < 2$ ) should be multiplied to  $\gamma$  for periodic optical waveguides, leading to the definition of the effective nonlinear parameter as

$$\gamma_{\text{eff}}^{\text{PC}} = \frac{k_0 n_2}{A_{\text{eff}}^{\text{PC}}} S^\xi, \quad (18)$$

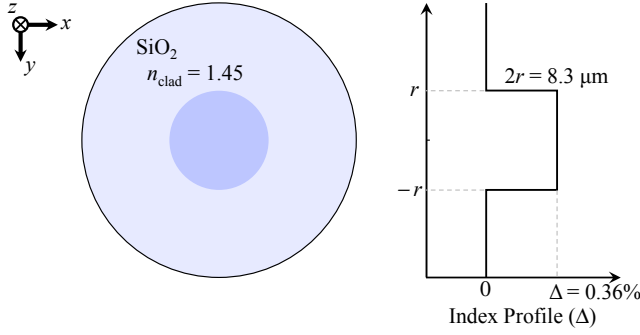


Fig. 2. Cross-section of the optical fiber and the refractive index profile.

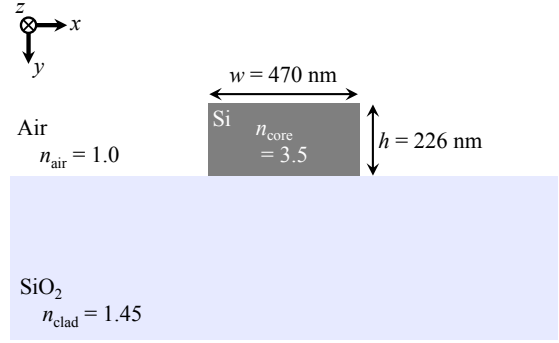


Fig. 3. Cross-section of the Si-nanowire waveguide on the SiO<sub>2</sub> layer.

**Table 2. Summary of  $\gamma$  and  $A_{\text{eff}}$  obtained by various methods for optical fibers**

|  | Value   |              |
|--|---|--------------|
| Wavelength $\lambda$ [ $\mu\text{m}$ ]                 | 1.550   | 1.310        |
| Effective index $n_{\text{eff}} (= \beta\lambda/2\pi)$ | 1.4523  | 1.4529       |
| Group index $n_g (= d\beta/dk_0)$                      | 1.4557  | 1.4559       |
| Slowdown factor $S (= n_g/n_{\text{core}})$            | 1.0003  | 1.0005       |
| Calculation Method                                     | Value of $\gamma$ [ $\text{km}^{-1}\text{W}^{-1}$ ] ( $A_{\text{eff}}$ [ $\mu\text{m}^2$ ]) |              |
| Method A (proposed)                                    | 1.16* (76.7)  | 1.70* (62.0) |
| Method B   | 1.16* (77.1)  | 1.69* (62.3) |
| Method C   | 2.30* (38.8)  | 3.23* (32.6) |
| Method E   | 1.16* (76.7)  | 1.70* (62.0) |
| Method F (measured) [27]                               | 1.09  | -            |

\*  $n_2$  is assumed as  $2.2 \times 10^{-20} \text{ m}^2\text{W}^{-1}$

**Table 3. Summary of  $\gamma$  and  $A_{\text{eff}}$  obtained by various methods for the Si-nanowire waveguide**

|  | Value  |         |
|--|--|---------|
| Wavelength $\lambda$ [ $\mu\text{m}$ ]                 | 1.550  | 1.550   |
| Effective index $n_{\text{eff}} (= \beta\lambda/2\pi)$ | 2.437  | 2.437   |
| Group index $n_g (= d\beta/dk_0)$                      | 4.283  | 4.283   |
| Slowdown factor $S (= n_g/n_{\text{core}})$            | 1.224  | 1.224   |
| Calculation Method                                     | Value of $\gamma$ [ $\text{m}^{-1}\text{W}^{-1}$ ] ( $A_{\text{eff}}$ [ $\mu\text{m}^2$ ]) |         |
| Method A (proposed)                                    | 190~910*   | (0.067) |
| Method B   | 63~300*  | (0.20)  |
| Method C   | 220~1100*  | (0.076) |
| Method E   | 190~910*   | (0.067) |
| Method F (measured) [7]                                | 200~2100   | -       |

\*  $n_2$  is assumed as a range of  $3.0 \times 10^{-18}$  to  $14.5 \times 10^{-18} \text{ m}^2\text{W}^{-1}$

$$\gamma_{\text{eff}}^{\text{eff}} = \frac{k_0 n_2}{A_{\text{eff}}^{\text{eff}}} S^\xi. \quad (19)$$

In Eqs. (18) and (19), Eqs. (15) and (17) are used for  $A_{\text{eff}}$ , and  $\xi$  is usually 2 [11,23,24,26]. In this paper,  $\xi = 2$  unless otherwise noted.

### E. $\gamma$ Calculated by Nonlinear Modal Analysis.

We proposed a method to directly estimate the nonlinear parameter using the 3D-FEM for nonlinear periodic optical waveguides, based on the self-consistent algorithm [19]. The nonlinear parameter and effective area obtained by the nonlinear modal analysis are defined as

$$\gamma^{\text{NLmode}} = \frac{|\beta_{\text{NL}} - \beta_{\text{L}}|}{P}, \quad (20)$$

$$A_{\text{eff}}^{\text{NLmode}} = \frac{k_0 n_2}{\gamma^{\text{NLmode}}}, \quad (21)$$

where  $\beta_{\text{L}}$  is the linear propagation constant, and  $\beta_{\text{NL}}$  is the nonlinear propagation constant for optical power  $P$ . For sufficiently small  $P$ , the nonlinear phase shift is proportional to  $P$ , and we can obtain constant  $\gamma$ . Although this method seems to give a physically correct  $\gamma$ , iterations are necessary to obtain converged solutions.

### F. Estimation of $\gamma$ by Experimental Value.

To estimate the nonlinear parameter and effective area from experimental results, conventionally, the following equation has been used [14]:

$$\gamma^{\text{Measured}} = \frac{\Delta\phi_{\text{max}}}{P_{\text{in}} L_{\text{eff}}}, \quad (22)$$

where  $\Delta\phi_{\text{max}}$  is the observed maximum nonlinear phase shift by SPM,  $P_{\text{in}}$  is the input optical power, and  $L_{\text{eff}}$  is the effective length given as  $[1 - \exp(-\alpha L)]/\alpha$  with the attenuation coefficient  $\alpha$  and propagation length  $L$ . The number of observed peaks  $m$  by SPM-induced spectral broadening is related to  $\Delta\phi_{\text{max}} = (m - 0.5)\pi$  [5].

In the following, we compare the  $\gamma$  values of various waveguides calculated by the above five methods, namely, Method A in Section 2-A, Method B in Section 2-B, Method C in Section 2-C, Methods D-1 and D-2 in Section 2-D, and Method E in Section 2-E with measured values and show that our proposed Method A and the nonlinear modal analysis in Section 2-E give reasonable results.

## 3. NUMERICAL ANALYSIS AND DISCUSSION

We demonstrate the validity of our proposed method by calculating the nonlinear parameter  $\gamma$  of an optical fiber, a Si-nanowire, and dispersion engineered PC waveguides. To avoid confusion, we call each method "Method A, B, C, D-1, D-2, E and F", and the descriptions and equations are summarized in Table 1. The 3D finite-element mode-solver [19] developed in our laboratory is used. For Methods A, B, C, D-1, and D-2, the analysis can also be done by using commercial software. Although the optical fiber and Si-wire waveguide are uniform along the

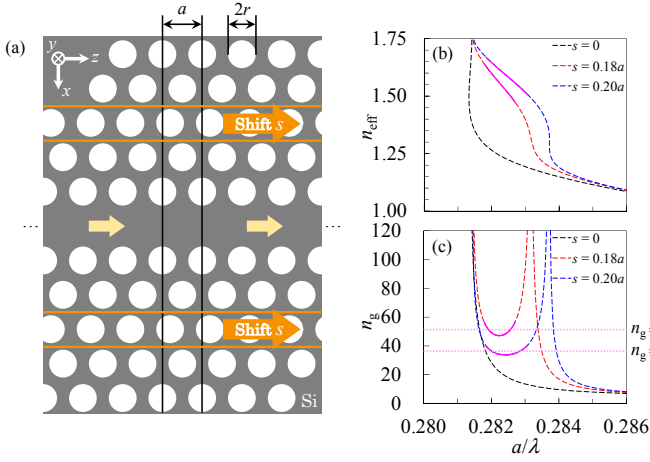


Fig. 4. (a) Schematics of the dispersion engineered PC waveguide with air cladding [28]. (b)  $\lambda$ - $n_{\text{eff}}$  curves and (c)  $\lambda$ - $n_g$  curves where  $s=0$  (black dashed lines),  $0.18a$  (red dashed lines),  $0.20a$  (blue dashed lines). Purple lines denote the flat band defined as a  $\pm 10\%$  change of  $n_g$ .

**Table 4. Summary of  $\gamma$ ,  $\gamma_{\text{eff}}$  and  $A_{\text{eff}}$  obtained by various methods for the dispersion engineered PC waveguide ( $s = 0.20a$ )**

|  | Value  |  |
|--|--|--|
| Normalized Frequency ( $= a/\lambda$ )                     | 0.282, 0.283   |  |
| Effective index $n_{\text{eff}}$ ( $= \beta\lambda/2\pi$ ) | 1.51, 1.67   |  |
| Group index $n_g$ ( $= d\beta/dk_0$ )                      | 36   |  |
| Slowdown factor $S$ ( $= n_g/n_{\text{core}}$ )            | 10.29  |  |
| Calculation Method   | Value of $\gamma$ [ $\text{m}^{-1}\text{W}^{-1}$ ] ( $A_{\text{eff}}$ [ $\mu\text{m}^2$ ]) |  |
| Method A (proposed)  | 4200~27000* (0.0022, 0.0029)   |  |
| Method B   | 24~115* (0.65, 0.86)   |  |
| Method C   | 130~780* (0.075, 0.093)  |  |
| Method D-1 ( $\gamma_{\text{eff}}$ )                       | 1500~9500* -   |  |
| Method D-2 ( $\gamma_{\text{eff}}$ )                       | 14000~82000* -   |  |
| Method E   | 4300~26000* (0.0023, 0.0028)   |  |
| Method F (measured) [28]                                   | 17000~34000 -  |  |

\*  $n_2$  is assumed as a range of  $3.0 \times 10^{-18}$  to  $14.5 \times 10^{-18} \text{ m}^2\text{W}^{-1}$

$z$ -direction, we can also treat them as periodic waveguides with no structural variations.

First, we examine the standard step-index optical fiber, as shown in Fig. 2. The structural parameters are the following: the core diameter is  $2r = 8.3 \mu\text{m}$ , the refractive indices of the core and cladding are  $n_{\text{core}} = 1.4552$  and  $n_{\text{clad}} = 1.4500$  (relative refractive index  $\Delta = (n_{\text{core}}^2 - n_{\text{clad}}^2) / (2n_{\text{core}}^2) = 0.36\%$ ), and the nonlinear refractive index of all materials is  $n_2 = 2.2 \times 10^{-20} \text{ m}^2\text{W}^{-1}$ . In Table 2,  $\gamma$  and  $A_{\text{eff}}$  obtained by various methods are summarized. The values calculated by Method A agree with those by Method B because the optical fiber is a weakly guiding structure. The calculated  $A_{\text{eff}}$  values by Methods A, B and E are approximately  $80 \mu\text{m}^2$  at  $\lambda (= 2\pi/k_0) = 1.550 \mu\text{m}$ , which is the  $A_{\text{eff}}$  value of the standard step-index fiber. However, the calculated  $A_{\text{eff}}$  value by Method C is half of those by Methods A, B and E.  $\gamma$  values calculated by Methods A, B and E agree well with the measured value [27], indicating the validity of Methods A and E. Here, Method D is omitted because  $S$  is almost 1.

Next, we examine the Si-nanowire waveguide, as shown in Fig. 3. The structural parameters are the following: the core width is  $w = 470 \text{ nm}$ , the core height is  $h = 226 \text{ nm}$ , and the refractive indices of Si (core),  $\text{SiO}_2$  (lower cladding), and air (upper cladding) are  $n_{\text{core}} = 3.5$ ,  $n_{\text{clad}} = 1.45$ , and  $n_{\text{air}} = 1.0$ . We assume a range of  $n_2$  for Si from  $3.0 \times 10^{-18}$  to  $14.5 \times 10^{-18} \text{ m}^2\text{W}^{-1}$  [10], and  $n_2$  of the cladding materials is neglected. In Table 3, the  $\gamma$  and  $A_{\text{eff}}$  values obtained by various methods are

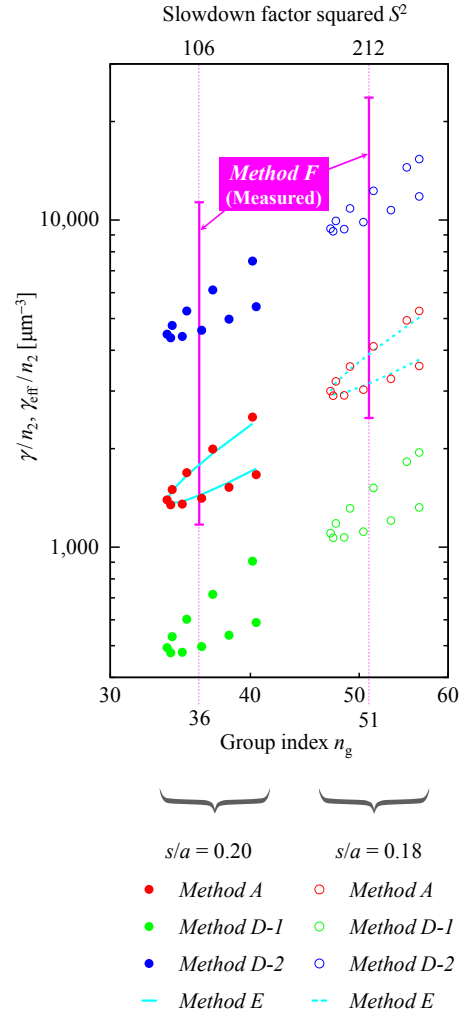


Fig. 5. Comparison of  $\gamma/n_2$  and  $\gamma_{\text{eff}}/n_2$  by various methods on the flat band in dispersion engineered PC waveguides for  $s = 0.18a$  (open circles and dashed line) and  $0.20a$  (closed circles and solid line). Red circles, green circles, blue circles, and cyan lines correspond to Method A, D-1, D-2, and E, respectively. Purple lines denote experimental values obtained by Method F in a similar structure for  $n_g = 36$  and 51.

summarized. The values calculated by Method A differ from those by Method B because the waveguide is strongly guiding ( $\Delta = 41\%$ ) and the weakly guiding approximation cannot hold. In contrast to the case of the optical fiber, the value calculated by Method C is close to that by Method A for the Si-nanowire. Therefore, Method B is not appropriate for strongly guiding structures, and the  $\gamma$  values calculated by Methods A, C and E agree well with the measured value [7]. Here, Method D is also omitted because  $S \approx 1$ .

Finally, we investigate the dispersion engineered PC waveguide [28–30], as shown in Fig. 4(a). The waveguide is designed to enhance the nonlinearity by causing flat- $n_g$  dispersion. The structural parameters are as follows: the lattice constant is  $a = 440 \text{ nm}$ , the hole radius is  $r = 0.35a$ , the thickness of the waveguide is  $t = 0.5a$ , the amount of the shift of the third-row holes along the  $z$ -direction is  $s = 0.18a$  or  $0.20a$ , and the refractive indices of the Si (core) and air (cladding) are  $n_{\text{core}} = 3.5$  and  $n_{\text{air}} = 1.0$ , respectively. We assume a range of  $n_2$  for Si from  $3.0 \times 10^{-18}$  to  $14.5 \times 10^{-18} \text{ m}^2\text{W}^{-1}$  [10], and  $n_2$  of the cladding material is neglected. Figures 4 (b) and (c) show the effective index  $n_{\text{eff}}$  and the group index  $n_g$  as a function of  $a/\lambda$ . By introducing hole shift, a flat- $n_g$  band is formed, as reported in [28]. The purple solid lines in the graphs denote the flat band region, in which the value of  $n_g$

changes  $\pm 10\%$ . In Table 4, the  $\gamma$ ,  $\gamma_{\text{eff}}$  and  $A_{\text{eff}}$  obtained by various methods of the PC waveguide for  $s=0.20a$  are summarized. There are two frequencies for  $n_g=36$  when  $s=0.20$ , as shown in Fig. 4 (c). For each frequency,  $\gamma$  has its range determined by the range of  $n_g$ . The maximum and minimum  $\gamma$  values are employed for the range of  $\gamma$  in Table 4.

The calculated  $\gamma$  value by Method A is approximately 200 times larger than that by Method B and 30 times larger than that by Method C. As in the previous two examples, the results obtained by Methods A and E agree well, and they are consistent with the measured values. Methods B and C are not appropriate for evaluating the  $\gamma$  of PC waveguides.

In the following, we discuss the results obtained by Methods D-1 and D-2 because the slowdown factor is very large ( $S=10.29$ ) and  $\gamma_{\text{eff}}$  is 100 ( $\approx S^2$ ) times larger than  $\gamma$ . Figure 5 shows that  $\gamma/n_g$  and  $\gamma_{\text{eff}}/n_g$  as a function of  $n_g$  obtained by various methods of dispersion engineered PC waveguides for  $s=0.18a$  ( $n_g \approx 51$ ) and  $0.20a$  ( $n_g \approx 36$ ). In this graph, numerical values only for the flat band region are displayed (corresponding to the purple solid lines in Fig. 4). Methods A, D-1, D-2, E, and F have roughly  $n_g^{-2}$  dependency, which implies that Method B and C have no dependence on  $n_g$  because  $S^2$  dependence is not introduced. As seen in Fig. 5, the calculated values obtained by Methods A, E and D-2 roughly agree with the measured values.  $\gamma_{\text{eff}}$  calculated by Method D-1 ( $A_{\text{eff}}$  is obtained by Method B) is relatively smaller than the measured values. In Method D,  $\xi=2$  is conventionally used to estimate the maximum nonlinearity where  $\xi$  ( $1 < \xi < 2$ ) is a fitting parameter. When  $\xi \approx 1.5$ , the calculated  $\gamma_{\text{eff}}$  values obtained by Method D-2 fit the  $\gamma$  values obtained Methods A and E.

Although Method D-2 gives reasonable  $\gamma_{\text{eff}}$  compared with the measured values for dispersion engineered PC waveguides, the value of  $\xi$  is usually unknown and requires fitting from measured values. Contrary to this, our proposed Methods A and E give reasonable  $\gamma$  without fitting parameters, such as slowdown factor  $S$ . Furthermore, from the results in this section, only Methods A and E give reasonable  $\gamma$  compared with the experiments for all three waveguide structures, showing the validity and versatility of the proposed  $\gamma$  and  $A_{\text{eff}}$  definitions. Additionally, Method A does not require the iteration of Method E, and the required computational cost is lower than that of Method E.

#### 4. CONCLUSION

In this paper, we have proposed a definition for the nonlinear parameter  $\gamma$  for HIC periodic optical waveguides, and the  $\gamma$  values obtained by the proposed and conventional definitions are compared with those obtained by the nonlinear guided mode analysis and the experiment for three waveguide structures. Our proposed  $\gamma$  (Method A) obtained from the derivation of vectorial-based NLSE is rigorous due to the exclusion of the weakly guiding approximation and an appropriate consideration of the variations of  $A_{\text{eff}}$  along the propagation direction. For the dispersion engineered PC waveguides analyzed here, the value of  $\gamma$  obtained by using the weakly guiding approximation (Method B) is 200 times smaller than that of the proposed definition. The results obtained by the proposed definition and the nonlinear guided mode analysis agree well, and the proposed method does not require iteration because only linear guided mode analysis is necessary. Furthermore, our proposed  $\gamma$  is also in good agreement with the experimental values for all three waveguides, as shown in Section 3. These results indicate that our proposed  $\gamma$  and  $A_{\text{eff}}$  are indispensable for HIC periodic waveguides and strongly encourage the use of Eq. (8) or Eqs. (10) and (11) for the appropriate calculation of nonlinear characteristics in future research.

#### References

1. N. Broderick, G. Ross, H. Offerhaus, D. Richardson, and D. Hanna, "Hexagonally poled lithium niobate: A two-dimensional nonlinear photonic crystal," *Phys. Rev. Lett.* **84**, 4345–4348 (2000).
2. S. Buckley, M. Radulaski, K. Biermann, and J. Vučković, "Second harmonic generation in photonic crystal cavities in (111)-oriented GaAs," *Appl. Phys. Lett.* **103**, 1–4 (2013).
3. R. S. Jacobsen, K. N. Andersen, P. I. Borel, J. Fage-Pedersen, L. H. Frandsen, O. Hansen, M. Kristensen, A. V. Lavrinenko, G. Moulin, H. Ou, C. Peucheret, B. Zsigri, and A. Bjarklev, "Strained silicon as a new electro-optic material," *Nature* **441**, 199–202 (2006).
4. J.-M. Brosi, C. Koos, L. C. Andreani, M. Waldow, J. Leuthold, and W. Freude, "High-speed low-voltage electro-optic modulator with a polymer-infiltrated silicon photonic crystal waveguide," *Opt. Express* **16**, 4177–4191 (2008).
5. R. H. Stolen and C. Lin, "Self-phase-modulation in silica optical fibers," *Phys. Rev. A* **17**, 1448–1453 (1978).
6. O. Boyraz, T. Indukuri, and B. Jalali, "Self-phase-modulation induced spectral broadening in silicon waveguides," *Opt. Express* **12**, 829–834 (2004).
7. E. Dulkeith, Y. A. Vlasov, X. Chen, N. C. Panoiu, and R. M. Osgood, Jr., "Self-phase-modulation in submicron silicon-on-insulator photonic wires," *Opt. Express* **14**, 5524–5534 (2006).
8. Q. Lin, O. J. Painter, and G. P. Agrawal, "Nonlinear optical phenomena in silicon waveguides: modeling and applications," *Opt. Express* **15**, 16604–16644 (2007).
9. M. A. Foster, A. C. Turner, M. Lipson, and A. L. Gaeta, "Nonlinear optics in photonic nanowires," *Opt. Express* **16**, 1300–1320 (2008).
10. H. K. Tsang and Y. Liu, "Nonlinear optical properties of silicon waveguides," *Semicond. Sci. Technol.* **23**, 064007–1–064007–9 (2008).
11. C. Monat, B. Corcoran, M. Ebnali-Heidari, C. Grillet, B. J. Eggleton, T. P. White, L. O'Faolain, and T. F. Krauss, "Slow light enhancement of nonlinear effects in silicon engineered photonic crystal waveguides," *Opt. Express* **17**, 2944–2953 (2009).
12. C. Husko, S. Combré, Q. V. Tran, F. Raineri, C. W. Wong, and A. D. Rossi, "Non-trivial scaling of self-phase modulation and three-photon absorption in III-V photonic crystal waveguides," *Opt. Express* **17**, 22442–22451 (2009).
13. J. Leuthold, C. Koos, and W. Freude, "Nonlinear silicon photonics," *Nat. Photonics* **4**, 535–544 (2010).
14. G. P. Agrawal, *Nonlinear Fiber Optics*, 5th ed. (Academic Press, 2012).
15. N. Matsuda, T. Kato, K. Harada, H. Takesue, E. Kuramochi, H. Taniyama, and M. Notomi, "Slow light enhanced optical nonlinearity in a silicon photonic crystal coupled-resonator optical waveguide," *Opt. Express* **19**, 19861–19874 (2011).
16. C. Koos, L. Jacome, C. Poulton, J. Leuthold, and W. Freude, "Nonlinear silicon-on-insulator waveguides for all-optical signal processing," *Opt. Express* **15**, 5976–5990 (2007).
17. M. Ebnali-Heidari, C. Monat, C. Grillet, and M. K. Moravvej-Farshi, "A proposal for enhancing four-wave mixing in slow light engineered photonic crystal waveguides and its application to optical regeneration," *Opt. Express* **17**, 18340–18353 (2009).
18. T. Fujisawa and M. Koshiba, "Guided modes of nonlinear slot waveguides," *IEEE Photonics Technol. Lett.* **18**, 1530–1532 (2006).
19. T. Sato, S. Makino, Y. Ishizaka, T. Fujisawa, and K. Saitoh, "Three-dimensional finite-element mode-solver for nonlinear periodic optical waveguides and its application to photonic crystal waveguides," *J. Lightw. Technol.* **32**, 4011–4019 (2014).
20. T. F. Krauss, "Slow light in photonic crystal waveguides," *J. Phys. D: Appl. Phys.* **40**, 2666–2670 (2007).
21. J. S. Foresi, P. R. Villeneuve, J. Ferrera, E. R. Thoen, G. Steinmeyer, S. Fan, J. D. Joannopoulos, L. C. Kimerling, H. I. Smith, and E. P. Ippen, "Photonic-bandgap microcavities in optical waveguides," *Nature* **390**, 143–145 (1997).
22. M. Notomi, "Manipulating light with strongly modulated photonic crystals," *Reports Prog. Phys.* **73**, 096501–1–096501–57 (2010).

23. C. Monat, B. Corcoran, D. Pudo, M. Ebnali-Heidari, C. Grillet, M. D. Pelusi, D. J. Moss, B. J. Eggleton, T. P. White, L. O'Faolain, and T. F. Krauss, "Slow light enhanced nonlinear optics in silicon photonic crystal waveguides," *IEEE J. Sel. Top. Quantum Electron.* **16**, 344–356 (2010).
24. S. Makino, Y. Ishizaka, K. Saitoh, and M. Koshiba, "Slow-light-enhanced nonlinear characteristics in slot waveguides composed of photonic crystal nanobeam cavities," *IEEE Photonics J.* **5**, 2700309–1–2700309–10 (2013).
25. T. Sato, S. Makino, Y. Ishizaka, and K. Saitoh, "Investigation of nonlinear characteristics in a 1-D slotted photonic crystal coupled resonator optical waveguide with modulated mode-gap," in *Optical Fibre Technology, 2014 OptoElectronics and Communication Conference and Australian Conference on* (2014), pp. 673–675.
26. J. F. McMillan, M. Yu, D.-L. Kwong, and C. W. Wong, "Observation of four-wave mixing in slow-light silicon photonic crystal waveguides," *Opt. Express* **18**, 15484–15497 (2010).
27. A. Boskovic, S. V. Chernikov, J. R. Taylor, L. Gruner-Nielsen, and O. A. Levring, "Direct continuous-wave measurement of  $n_2$  in various types of telecommunication fiber at 1.55  $\mu\text{m}$ ," *Opt. Lett.* **21**, 1966–1968 (1996).
28. M. Shinkawa, N. Ishikura, Y. Hama, K. Suzuki, and T. Baba, "Nonlinear enhancement in photonic crystal slow light waveguides fabricated using CMOS-compatible process.," *Opt. Express* **19**, 22208–22218 (2011).
29. K. Suzuki, Y. Hamachi, and T. Baba, "Fabrication and characterization of chalcogenide glass photonic crystal waveguides," *Opt. Express* **17**, 22393–22400 (2009).
30. K. Suzuki and T. Baba, "Nonlinear light propagation in chalcogenide photonic crystal slow light waveguides.," *Opt. Express* **18**, 26675–26685 (2010).